

# Enhanced anticancer effect of oncostatin M combined with salinomycin in CD133<sup>+</sup> HepG2 liver cancer cells

CHANGHAO FU<sup>1\*</sup>, LU WANG<sup>1\*</sup>, GEER TIAN<sup>1</sup>, CHEN ZHANG<sup>1,2</sup>, YUANYUAN ZHAO<sup>1</sup>,  
HAO XU<sup>1</sup>, MANMAN SU<sup>1</sup> and YI WANG<sup>1</sup>

<sup>1</sup>Department of Regenerative Medicine, School of Pharmaceutical Sciences, Jilin University, Changchun, Jilin 130021;

<sup>2</sup>Xiamen Institute of Rare Earth Materials, Chinese Academy of Sciences, Xiamen, Fujian 361021, P.R. China

Received March 14, 2018; Accepted November 2, 2018

DOI: 10.3892/ol.2018.9796

**Abstract.** Oncostatin M (OSM) induces the differentiation of liver cancer stem cells (LCSCs) and increases sensitivity to the chemotherapeutic agent 5-fluorouracil, whereas salinomycin (Sal) induces apoptosis in cancer stem cells and inhibits the proliferation of liver cancer cells. However, there have been no studies investigating the anticancer effects of combination treatment with OSM and Sal. In the present study, we investigated the synergistic effects of OSM and Sal on LCSCs, the CD133<sup>+</sup> subpopulations from HepG2 human liver cancer cells. CD133<sup>+</sup>LCSCs were isolated using an immunomagnetic bead technique and identified through colony formation. After incubating with OSM and Sal, the ability of LCSC proliferation and invasion, as well as apoptosis rates were evaluated, and the expression of stemness-related genes was examined by quantitative real-time polymerase chain reaction. Additionally, the secretion of  $\alpha$ -fetoprotein (AFP) and albumin (ALB) were analyzed by enzyme-linked immunosorbent assay. Our results indicated that OSM combined with Sal significantly

suppressed LCSC proliferation and invasion and induced apoptosis, as determined by flow cytometry and increases in cleaved caspase-3 levels detected by western blotting. The results of the JC-1 staining assay indicated that this effect involved the mitochondrial pathway. Moreover, combination treatment reduced the expression of CD133 in LCSCs and suppressed stemness-related gene expression. Furthermore, the LCSCs produced lower levels of AFP and higher levels of ALB following combination treatment. In all experiments, combination treatment elicited more efficient anticancer effects on LCSCs as compared with single-drug treatment; therefore, our results demonstrated that combined treatment with OSM and Sal inhibited proliferation and induced differentiation and apoptosis in LCSCs, suggesting combined use of OSM and Sal as a therapeutic strategy for liver cancer.

## Introduction

Liver cancer is the third most common malignancy in China, accounting for an estimated 380,000 deaths annually and representing ~54% of liver cancer cases worldwide (1). Liver cancer is also the second most lethal cancer due in part to the resistance to conventional chemotherapeutic drugs and radiation therapy by a subpopulation of tumor cells referred to as cancer stem cells (CSCs). CSCs display distinct immunophenotypes and exhibit the capacity for unlimited self-renewal and heterogeneous-lineage differentiation into different cancer-cell types that comprise the tumor (2,3), making CSCs responsible for tumor initiation, propagation, and tumor heterogeneity. CSCs are more resistant to chemotherapy, and the inability to eradicate CSC populations results in tumor relapse and distant metastasis.

There are currently a significant number of anti-CSC drugs under investigation. Salinomycin (Sal) is a polyether ionophore antibiotic produced through fermentation by *Streptomyces albus* and that is widely used to treat coccidiosis (4). Following the report by Gupta *et al* (5) that Sal exhibits the ability to selectively deplete human breast CSCs from tumorspheres, several other groups have demonstrated that Sal inhibited cancer growth and induced apoptosis in different CSCs and cancer types, including liver cancer (6-9). Although the underlying mechanism associated with Sal acting as a chemotherapeutic drug for liver cancer remains unclear, a previous

---

*Correspondence to:* Professor Yi Wang or Professor Manman Su, Department of Regenerative Medicine, School of Pharmaceutical Sciences, Jilin University, 1266 Fujin Road, Changchun, Jilin 130021, P.R. China  
E-mail: wangyi@jlu.edu.cn  
E-mail: summ@jlu.edu.cn

\*Contributed equally

**Abbreviations:** 5-FU, 5-fluorouracil; bFGF, basic fibroblast growth factor; CCK-8, Cell Counting Kit-8; CSC, cancer stem cell; DMEM, Dulbecco's Modified Eagle's Medium; DMSO, dimethylsulfoxide; ELISA, enzyme-linked immunosorbent assay; EGF, epidermal growth factor; EpCAM<sup>+</sup>, epithelial cell adhesion molecule-positive; FBS, fetal bovine serum; FITC, fluorescein isothiocyanate; LCSC, liver cancer stem cell; OSM, oncostatin M; PBS, phosphate-buffered saline; PI, propidium iodide; RT-qPCR, reverse transcription-quantitative polymerase chain reaction; Sal, salinomycin

**Key words:** liver cancer, combinatorial treatment, apoptosis, differentiation, inhibition

study revealed that Sal reduced the proportion of CD133<sup>+</sup> cell subpopulations in the liver cancer cell line HepG2, inhibited liver cancer cell proliferation, suppressed cell cycle progression, and induced apoptosis by repressing intracellular Ca<sup>2+</sup> and the Wnt/ $\beta$ -catenin-signaling pathway (10). However, similar to breast cancer (11) and glioblastoma (4), phenotypic heterogeneity within CSC subpopulations may exist in liver cancer. Identification of the surface markers CD13, CD24, CD44, CD90, CD133, and epithelial-cell adhesion molecule (EpCAM) (12-14) in liver cancer cells indicates that heterogeneous LCSCs may not be targeted by a single CSC-specific drug. Therefore, it is necessary to eliminate LCSCs using a combinatorial treatment of Sal and another CSC-specific drug or a drug that may induce undifferentiated CSCs toward a more differentiated state in order to improve the efficacy of liver cancer treatment.

Oncostatin M (OSM), a cytokine of the interleukin-6 family, is a multifunctional cellular regulator produced by CD45<sup>+</sup> hematopoietic cells that induces the differentiation of hepatoblasts into hepatocytes in a distinct OSM-receptor-specific manner. Yamashita *et al* (12) reported the enhanced differentiation of EpCAM<sup>+</sup> liver cancer cells into hepatocytes via OSM-receptor signaling, where the OSM receptor is mainly expressed in hepatic stem/progenitor cells and rarely detected in hepatocytes (12). OSM was also revealed to induce hepatic differentiation through activation of the signal transducer and activator of transcription 3 pathway, as evidenced by decreased levels of  $\alpha$ -fetoprotein (AFP) and cytokeratin and increased albumin (ALB) levels in EpCAM<sup>+</sup> liver cancer cells (12). Furthermore, OSM stimulated tissue regeneration and reconstruction, prevented hepatocyte apoptosis, and regulated lipid metabolism, thereby rendering it potentially useful in preventing or treating liver injury (15). In fact, OSM alleviated liver injury in mice by inducing the differentiation of bone marrow mesenchymal stem cells into liver cells (16,17). Sal and OSM have each demonstrated anti-CSC effects in different ways; however, to the best of our knowledge, the synergistic effects of OSM and Sal have not been previously investigated. To address this issue, we examined the anticancer effects of OSM combined with Sal on CD133<sup>+</sup> LCSCs. Our results demonstrated the enhanced anticancer effects of the combined treatment as evidenced by increased apoptosis, reduced proliferation, and enhanced differentiation of LCSCs when compared with results observed from treatment with Sal or OSM alone.

## Materials and methods

**Cell line and culture.** HepG2 human liver cancer cells were purchased from the Cell Bank of the Chinese Academy of Sciences (Shanghai, China) and were cultured in high-glucose Dulbecco's modified Eagle medium (DMEM; Gibco; Thermo Fisher Scientific, Inc., Waltham, MA, USA) supplemented with 10% fetal bovine serum (FBS; Gibco; Thermo Fisher Scientific, Inc.) at 37°C and 5% CO<sub>2</sub>.

**Magnetic-activated cell sorting.** Briefly, HepG2 cells were harvested and incubated with the anti-CD133 monoclonal antibody conjugated to biotin (Miltenyi Biotec, Inc., Auburn, CA, USA) for 10 min at 4°C, followed by fractionation using

a CELlection Biotin Binder kit (Invitrogen; Thermo Fisher Scientific, Inc.) according to the manufacturer's instructions. The sorted CD133<sup>+</sup> HepG2 cells were cultured in DMEM/F12 (Gibco; Thermo Fisher Scientific, Inc.) supplemented with 20 ng/ml epidermal growth factor (EGF) and 20 ng/ml basic fibroblast growth factor (bFGF; both from PeproTech, Inc., Rocky Hill, NJ, USA), and 2% B27 (Gibco; Thermo Fisher Scientific, Inc.) at 37°C and 5% CO<sub>2</sub>.

**Tumorsphere-formation assay.** Briefly, the sorted CD133<sup>+</sup> HepG2 cells were cultured in serum-free DMEM/F12 medium supplemented with 20 ng/ml EGF, 20 ng/ml bFGF, and 2% B27. Cells were then seeded on uncoated 6-well culture plates (Corning, Inc., Corning, NY, USA) at a density of 1x10<sup>4</sup> cells/well, with fresh medium added every 3 days (18). Tumorsphere formation was observed and images were captured using an inverted light microscope (Olympus Corporation, Tokyo, Japan).

**Analysis of serum-induced differentiation.** Cells were resuspended and incubated in DMEM/F12 supplemented with 10% FBS at 37°C and 5% CO<sub>2</sub>. Images of the cells were acquired using an inverted light microscope (Olympus Corporation).

**Soft-agar colony formation assay.** The 0.5% liquid soft agar was prepared by mixing 5% agar in phosphate-buffered saline (PBS) with culture medium (37°C), followed by transfer to a 6-well plate (1.5 ml/well) for solidification at room temperature. Subsequently, the cells mixed with 0.3% liquid agar were seeded in the solidified agar-based 6-well plate at 100 cells/well and cultured for 21 days at 37°C and 5% CO<sub>2</sub>. Images were acquired every 3 days using an optical light microscope (Olympus Corporation).

**Flow cytometric detection of cell-surface markers.** HepG2 cells and LCSCs were dissociated into single cells, and LCSCs were prepared at a concentration of 2.0x10<sup>5</sup> cells in 0.1 ml of PBS. The fluorescein isothiocyanate (FITC)-conjugated anti-CD133 antibody (1: 20; cat. no. 11-1339-42; Invitrogen; Thermo Fisher Scientific, Inc.) was added to the cell suspension, which was subsequently incubated in the dark for 30 min at 4°C. After two washes in PBS, the cells were acquired and analyzed by a flow cytometer (Beckman Coulter, Brea, CA, USA) in order to quantify the number of CD133<sup>+</sup> cells.

**Cell Counting Kit-8 (CCK-8) assay.** First, LSCSs (1x10<sup>5</sup>/well) were seeded in each well of a 96-well plate, with 100  $\mu$ l of medium in each well. Following incubation for 24 h, OSM was added at different concentrations (0, 1, 10 and 100 ng/ml). Triplicate samples were developed for each concentration. Cell viability was assessed at 48, 96 and 144 h using a CCK-8 kit (Beyotime Institute of Technology, Haimen, China) according to the manufacturer's instructions. LSCSs (1x10<sup>5</sup> cells/well) were also seeded in 96-well plates for 24 h and treated with a series of concentrations of Sal (0, 1, 2, 5, 10, 15, 20 and 25  $\mu$ M) in triplicate per concentration. After incubation for 24, 48 and 72 h, cell viability was detected using a CCK-8 kit.

Subsequently, the cytotoxicity of OSM, Sal, and OSM + Sal was measured via CCK-8 assay. Briefly, LCSCs (1x10<sup>5</sup> cells/well) were seeded in a 96-well plate containing

100  $\mu$ l of medium in each well and treated with OSM (10 ng/ml), followed by Sal (1  $\mu$ M) 3 days later. The total culture time was 6 days. Cells treated with 1  $\mu$ g/ml 5-fluorouracil (5-FU) served as positive controls, and culture medium was used as a negative control. Cell viability was determined by CCK-8 assay. Samples were processed in triplicate. Absorbance was measured at 450 nm using a Multiskan GO microplate reader (Thermo Fisher Scientific, Inc.). Cell viability was determined and the inhibition ratio was calculated using the following formula: Inhibition ratio (%)=(1-optical density of the treatment group/optical density of the solvent control) x100.

**Detection of apoptosis by Annexin V-FITC/propidium iodide (PI) staining.** Apoptotic cells were detected using an Annexin V/PI-FITC kit (Nanjing KeyGen Biotech Co., Ltd., Nanjing, China) according to the manufacturer's instructions. Briefly, cells were seeded in a 6-well plate (1x10<sup>6</sup> cells/well) and incubated with 10 ng/ml OSM, 1  $\mu$ M Sal, or both (10 ng/ml OSM + 1  $\mu$ M Sal) for 6 days at 37°C and 5% CO<sub>2</sub>, with 1  $\mu$ g/ml 5-FU and culture medium used as positive and negative controls, respectively. After washing with PBS, cells (5x10<sup>5</sup>) were resuspended in binding buffer (500  $\mu$ l) and stained with Annexin V-FITC (5  $\mu$ l) and PI (5  $\mu$ l) in the dark at room temperature for 5 min before analysis on a flow cytometer within 1 h. The experiment was repeated three times.

**JC-1 assay.** Mitochondrial membrane potential was detected by JC-1 staining assay using a kit (Nanjing KeyGen Biotech Co., Ltd.). Briefly, cells were seeded in a 6-well plate (1x10<sup>6</sup> cells/well) and incubated with 10 ng/ml OSM, 1  $\mu$ M Sal, or both (10 ng/ml OSM + 1  $\mu$ M Sal) for 6 days at 37°C and 5% CO<sub>2</sub>, with 1  $\mu$ g/ml 5-FU and culture medium used as positive and negative controls, respectively. After washing with PBS, the cells were resuspended in 500  $\mu$ l binding buffer, and 5x10<sup>5</sup> cells were stained with JC-1 (5  $\mu$ l) and PI (5  $\mu$ l) and incubated in the dark at room temperature for 15 min at 37°C and 5% CO<sub>2</sub>. The cells were then resuspended in incubation buffer (500  $\mu$ l) and analyzed by flow cytometry. The experiment was performed three times.

**Real-time reverse transcription-quantitative polymerase chain reaction (RT-qPCR).** LCSCs (1x10<sup>6</sup> cells/well) were plated in a 6-well plate and incubated with 10 ng/ml OSM, 1  $\mu$ M Sal, or both (10 ng/ml OSM + 1  $\mu$ M Sal) for 6 days at 37°C and 5% CO<sub>2</sub>, with 1  $\mu$ g/ml 5-FU and culture medium used as positive and negative controls, respectively. Total RNA was extracted using TRIzol reagent (Invitrogen; Thermo Fisher Scientific, Inc.), and first-strand cDNA was synthesized using a PrimeScript RT kit (Takara Bio, Inc., Otsu, Japan). Primers used for PCR are presented in Table I. cDNA was then used in qPCR reactions to analyze *NANOG*, *OCT4*, and *c-MYC* expression using FastStart SYBR Green master mix (Roche Diagnostics GmbH, Mannheim, Germany) in a 10- $\mu$ l reaction volume on a PikoReal 96 Real-Time PCR system (Thermo Fisher Scientific, Inc.). cDNA was denatured for 10 min at 95°C, and PCR was run for 45 cycles, with each cycle including steps of 5 sec at 95°C and 20 sec at 60°C. Polymerization of cDNA was performed for 10 min at 72°C, and 5-FU (1  $\mu$ g/ml) and culture medium were used as positive and negative controls, respectively. Experiments were

Table I. Primer sequences.

Target gene	Sequence (5'-3')	Product size, bp
28S	F: TTCACCAAGCGTTGGATTGTT R: TGTCTGAACCTGCGGTTCTT	146
OCT4	F: GCAGCTTGGGCTCGAGAAGGAT R: AGCCCAGAGTGGTGACGGAGAC	269
NANOG	F: CCTGATTCTTCCACCAGTCC R: TGCTATTCTTCGGCCAGTTG	292
c-MYC	F: CACCAGCAGCGACTCTGAGGAG R: ACTTGACCCTCTTGGCAGCAGG	239

F, forward; R, reverse.

performed in triplicate. Average CT values of the target genes were normalized to controls as  $\Delta\Delta Cq$  (19). The ratio of each gene against 28S levels was calculated by standardizing the ratio of each control to the unit value.

**Western blotting.** The expression of cleaved caspase-3 and total caspase-3 in LCSCs was evaluated by western blotting. Cells (1x10<sup>6</sup>/well) were seeded in a 6-well plate and incubated with 10 ng/ml OSM, 1  $\mu$ M Sal, or both (10 ng/ml OSM + 1  $\mu$ M Sal) for 6 days at 37°C and 5% CO<sub>2</sub>, with 1  $\mu$ g/ml 5-FU and culture medium used as positive and negative controls, respectively. Cells were lysed in 1 ml radioimmunoprecipitation buffer containing 10  $\mu$ l phenylmethylsulfonyl fluoride. Protein concentrations were determined with a bicinchoninic acid assay kit (Beyotime Institute of Biotechnology). The proteins (50  $\mu$ g each) were separated by 12% sodium dodecyl sulfate polyacrylamide gel electrophoresis at 160 V for 1 h, followed by transfer to a polyvinylidene difluoride membrane at 100 V for 1 h at room temperature. After blocking in 5% non-fat milk in Tris-buffered saline for 1 h, the membrane was incubated overnight at 4°C with anti-cleaved caspase-3 antibody (1:1,000; cat. no. 9664), anti-total caspase-3 antibody (1:1,000; cat. no. 9662) (both from Cell Signaling Technology, Inc., Danvers, MA, USA) and anti- $\beta$ -actin antibody (1:1,000; cat. no. sc-517582; Santa Cruz Biotechnology, Inc., Dallas, TX, USA), washed five times for 5 min each with Tris-buffered saline containing 0.5% Tween-20, and then incubated for 1 h at room temperature with horseradish peroxidase-conjugated secondary antibodies anti-rabbit IgG (1:5,000; cat. no. 7470) and anti-mouse IgG (1:3,000; cat. no. 7076) (both from Cell Signaling Technology, Inc.). The membrane was washed as previously described, and protein bands were visualized using X-ray film by enhanced chemiluminescence (GE Healthcare, Chicago, IL, USA).

**Transwell invasion assay.** An invasion assay was performed using 6.5-mm Transwell plates with sterile 8.0- $\mu$ m pore polycarbonate membrane inserts (Corning, Inc.) and covered with a thin layer of BD Matrigel (BD Biosciences, San Diego, CA, USA). Briefly, 1x10<sup>6</sup> cells/well were seeded in a Transwell plate and treated with 10 ng/ml OSM, 1  $\mu$ M Sal, or both

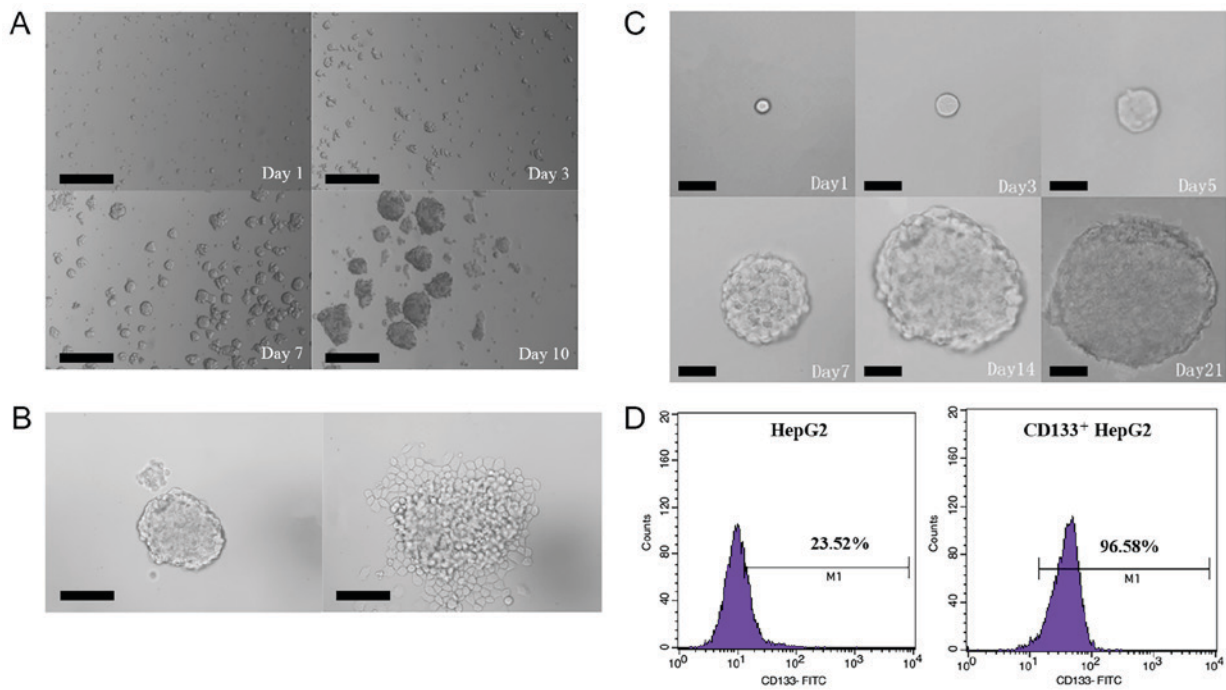


Figure 1. Isolation and characterization of CD133<sup>+</sup> LCSCs. (A) Optical micrographs presenting the morphology of LCSCs were obtained by magnetic-activated cell sorting over 10 days. Scale bar, 400  $\mu$ m. (B) Serum-induced differentiation of LCSCs into adherent cells. Scale bar, 100  $\mu$ m. (C) Growth and proliferation of LCSCs, and formation of colonies in soft agar over 21 days evaluated by soft-agar colony formation assay. Scale bar, 50  $\mu$ m. (D) LCSC percentage in HepG2 cells before and after magnetic-activated cell sorting evaluated by flow cytometry. LCSCs, liver cancer stem cells.

(10 ng/ml OSM + 1  $\mu$ M Sal), with 1  $\mu$ g/ml 5-FU and culture medium used as positive and negative controls, respectively. DMEM/F12 medium supplemented with 10% FBS was loaded into the bottom chamber through the insert as a chemostatic factor. After incubation for 6 days at 37°C and 5% CO<sub>2</sub>, the media in the upper and lower chambers were removed, and cells were fixed with 4% paraformaldehyde (500  $\mu$ l) for 20 min, washed twice with PBS (500  $\mu$ l), and stained with crystal violet (400  $\mu$ l) for 20 min. Cells were counted on an inverted light microscope, and the mean value was determined from counts of five random fields.

**Enzyme linked immunosorbent assay (ELISA).** Cells were seeded in a 6-well plate at 1x10<sup>6</sup>/well and incubated with 10 ng/ml OSM, 1  $\mu$ M Sal, or both (10 ng/ml OSM + 1  $\mu$ M Sal) for 6 days at 37°C and 5% CO<sub>2</sub>, with 1  $\mu$ g/ml 5-FU and culture medium used as positive and negative controls, respectively. AFP and ALB in the supernatant were detected by quantitative ELISA using kits (R&D Systems, Inc., Minneapolis, MN, USA) according to the manufacturer's instructions.

**Statistical analyses.** Data are presented as the means  $\pm$  standard deviation and analyzed using SPSS (v.17.0; SPSS, Inc., Chicago, IL, USA). One-way analysis of variance followed by a Tukey-Kramer multiple comparisons test were used to compare the corresponding data, and P<0.05 was considered to indicate a statistically significant difference.

## Results

**Isolation and characterization of CD133<sup>+</sup> HepG2 cells.** Prior to cell sorting, CD133 expression was analyzed

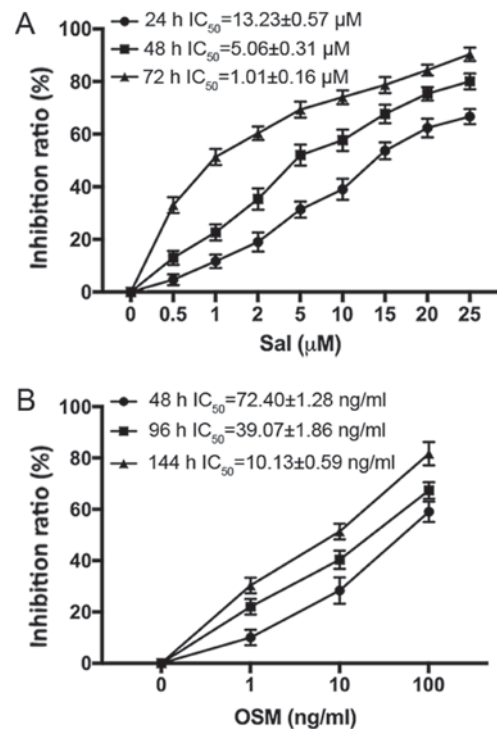


Figure 2. OSM and Sal reduce LCSC viability. (A and B) LCSCs treated with (A) Sal (0-25 mM) at 24, 48 and 72 h or (B) OSM (0, 1, 10 and 100 ng/ml) at 48, 96 and 144 h were assessed for cell viability using a CCK-8 assay. The data revealed that Sal and OSM reduced LCSCs in a concentration- and time-dependent manner. Data represent the means  $\pm$  standard deviation. OSM, oncostatin M; Sal, salinomycin; LCSC, liver cancer stem cell.

by flow cytometry in order to evaluate the proportion of CD133<sup>+</sup> cells in the liver cancer HepG2 cell line. The

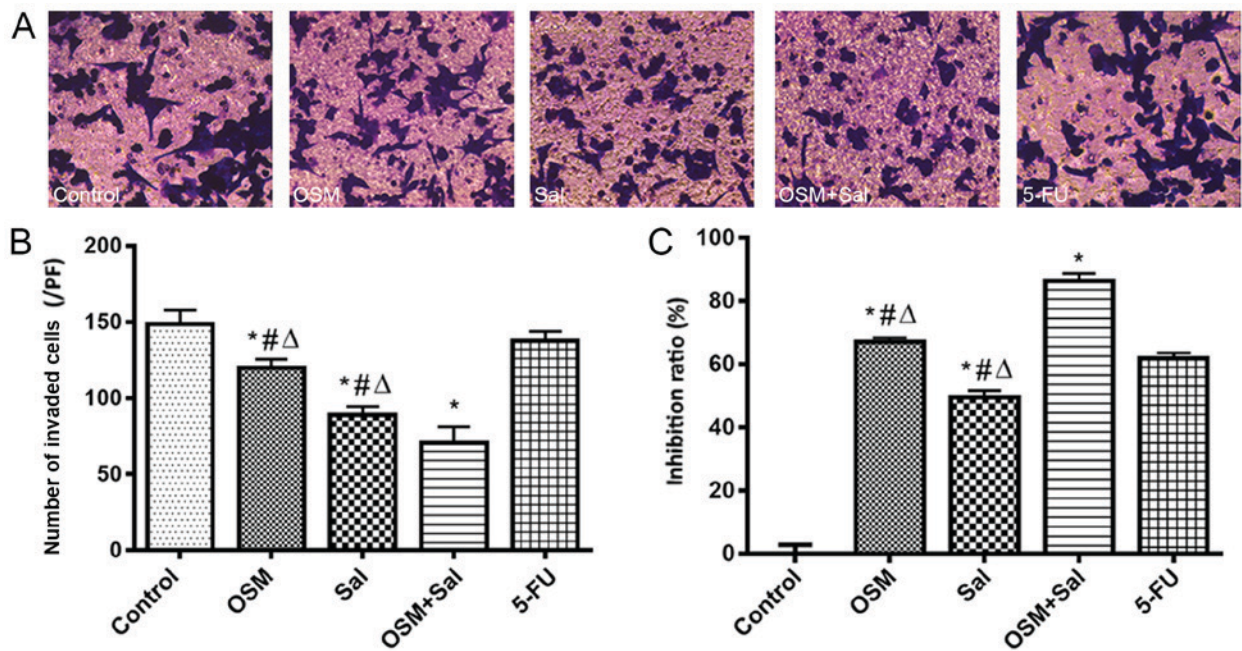


Figure 3. OSM and Sal inhibit LCSC proliferation and invasion. (A) Optical micrographs presenting the inhibition of LCSC invasiveness after treatment with OSM and Sal individually and in combination according to Transwell-migration assay. Magnification, x200. (B and C) Inhibition of LCSC (B) invasiveness and (C) proliferation following treatment with OSM and Sal individually and in combination. OSM (10 ng/ml), Sal (1  $\mu$ M), or both (10 ng/ml OSM + 1  $\mu$ M Sal) were used in the experiments. Cells treated with 1  $\mu$ g/ml 5-FU served as the positive controls, and culture medium was used as a negative control. Data represent the means  $\pm$  standard deviation. \* $P$ <0.05, compared with the control; # $P$ <0.05, compared with 5-FU;  $\Delta P$ <0.05, compared with the combination (OSM + Sal). OSM, oncostatin M; Sal, salinomycin; LCSC, liver cancer stem cell; 5-FU, 5-fluorouracil.

results revealed that CD133<sup>+</sup> cells accounted for 2.5% of unsorted HepG2 cells. To verify the stemness of CD133<sup>+</sup> HepG2 cells, tumorsphere formation, colony formation, and serum-induced differentiation assays were performed *in vitro*. In the tumorsphere-formation assay, the sorted CD133<sup>+</sup> HepG2 cells cultured in the serum-free DMEM/F12 medium grew in the form of suspended individual cells on Day 1 and began to aggregate into clusters on Day 3. As time passed, the small clusters gradually increased both in size and number and became visible to the naked eye on Day 10 (Fig. 1A). In the serum-induced differentiation assay, sorted CD133<sup>+</sup> HepG2 cells cultured for 7 days were resuspended in a basal medium supplemented with 10% FBS, resulting in a layer of adherent confluent cells on Day 3 (Fig. 1B). In the colony formation assay, CD133<sup>+</sup> HepG2 cells (100 cells/well) were inoculated onto soft agar, with small cell aggregates forming on Day 3 and micro-colonies detected on Day 5. Small colonies were visible to the naked eye on Day 7, and tumorspheres were observed after culturing for 21 days (Fig. 1C). Additionally, flow cytometric analyses revealed that before and after isolation by magnetic-activated cell sorting, 23.52 and 96.58% of cells, respectively, were CD133<sup>+</sup> (Fig. 1D).

**Sal and OSM treatment inhibits LCSC proliferation and migration.** Sal or OSM cytotoxicity was determined by CCK-8 assay. The IC<sub>50</sub> values of LCSCs at variable treatment times are presented in Fig. 2. The data indicated that Sal and OSM reduced LCSCs in a concentration- and time-dependent manner. According to the IC<sub>50</sub> values, 1  $\mu$ M Sal and 10 ng/ml OSM or both were used in the following experiments.

The combined treatment with OSM and Sal inhibited LCSC migration to a greater extent than Sal or OSM alone ( $P$ <0.05) according to Transwell-migration assay (Fig. 3A and B), indicating that OSM combined with Sal treatment effectively suppressed the malignant potential of LCSCs. Furthermore, CCK-8 assay revealed that combination (OSM + Sal) treatment exhibited a more potent suppressive effect on LCSC proliferation than either drug alone ( $P$ <0.05; Fig. 3C).

**Sal and OSM induce LCSC apoptosis.** Treatment with Sal, OSM, or both increased the percentage of Annexin V-positive LCSCs to 24.01, 13.13 and 40.16% of total cells, respectively, as compared with 12.71% in the 5-FU positive-control group ( $P$ <0.05; Fig. 4A). Additionally, JC-1 staining revealed that 59.26, 72.02 and 82.79% of cells exhibited a loss of mitochondrial membrane potential upon treatment with OSM, Sal, and OSM + Sal, respectively ( $P$ <0.05; Fig. 4B). Moreover, cleaved caspase-3 levels were higher and total caspase-3 were lower in cells treated with OSM + Sal than in those treated with the individual drugs according to western blot analysis ( $P$ <0.05; Fig. 4C and D). These results indicated that the combination drug treatment more potently induced apoptosis in LCSCs than either drug alone, and that this effect was likely mediated by the mitochondrial apoptosis pathway.

**Sal and OSM induce the expression of stem cell differentiation-related markers.** The fraction of LCSCs expressing CD133 after treatment with OSM, Sal, or both was 51.90, 61.31 and 36.48%, respectively, as compared with 97.20% for the blank control group and according to flow cytometric analysis. Therefore, combination treatment reduced the size of the CD133<sup>+</sup> population to a greater extent than individual drug

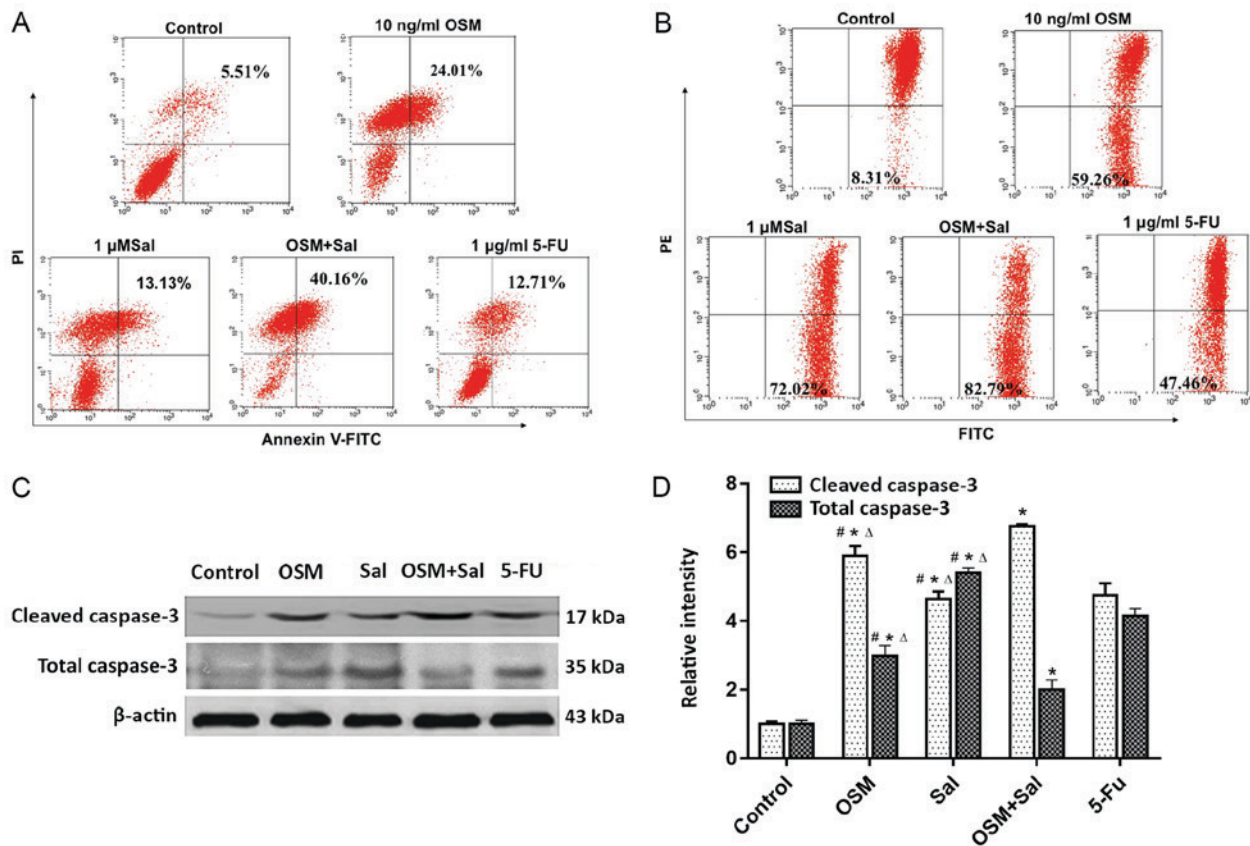


Figure 4. OSM and Sal induce LCSC apoptosis. (A) Flow cytometric analysis of Annexin V/PI staining of LCSCs treated with OSM and Sal individually and in combination. Dot plots show Annexin V/FITC and PI fluorescence staining. Lower-right and upper-right quadrants are apoptotic cells. (B) JC-1 staining assay following treatment of LCSCs with OSM and Sal individually and in combination. Apoptotic cells are shown in the lower-right quadrant of the dot plots. (C) Western blot analysis revealed total caspase-3 and cleaved caspase-3 levels following treatment of LCSCs with OSM and Sal individually and in combination. (D) Gray analysis of western blotting on total caspase-3 and cleaved caspase-3. OSM (10 ng/ml), Sal (1 μM), or both (10 ng/ml OSM + 1 μM Sal) were used in the experiments. Cells treated with 1 μg/ml 5-FU served as the positive controls, and culture medium was used as a negative control. Data represent the means ± standard deviation. \*P<0.05, compared with the control; #P<0.05, compared with 5-FU; ΔP<0.05, compared with the combination (OSM + Sal). OSM, oncostatin M; Sal, salinomycin; LCSC, liver cancer stem cell; PI, propidium iodide; FITC, fluorescein isothiocyanate; 5-FU, 5-fluorouracil.

treatments ( $P<0.05$ ; Fig. 5A). Additionally, real-time qPCR analysis revealed that *NANOG*, *c-MYC*, and *OCT4* levels were lower in cells treated with OSM + Sal than in those treated with Sal or OSM alone ( $P<0.05$ ; Fig. 5B). Moreover, the decrease in AFP secretion and the increase in ALB secretion were greater in cells receiving combination treatment as compared with the other experimental and 5-FU positive-control groups ( $P<0.05$ ; Fig. 5C and D). These results indicated that treatment with OSM combined with Sal potently suppressed the stemness characteristics of LCSCs.

## Discussion

CD133 is a prominent cell-surface marker used to identify CSCs. CD133 was originally found on hematopoietic stem/progenitor cells and neural stem cells and was subsequently reported to be expressed in CSCs from many types of malignancies, including brain, prostate, pancreatic, lung, and colon cancers (20). Recently, Ma *et al.* (21) reported CD133 as a potent CSC marker in liver cancer cell lines, including HepG2 and xenograft tumors. The CD133<sup>+</sup> subpopulation constitutes one of the most immature stages of liver cancer cells and is more resistant to conventional chemotherapeutic agents, such as 5-FU (21,22), due to the expression of genes

important for the self-renewal and proliferative properties of stem/progenitor cells. These genes include those encoding β-catenin involved in the Wnt-signaling pathway, which plays a critical role in cell proliferation, migration, and differentiation. In the present study, CD133 was used as a marker for the isolation of subsets enriched with CSCs from the liver cancer cell line HepG2 by magnetic-activated cell sorting, and it was revealed that CD133<sup>+</sup> HepG2 CSCs (termed LCSCs) accounted for 2.5% of all HepG2 cells, which was consistent with the range 1.16 to 4.37% reported previously (23). Therefore, this finding was in agreement with the hypothesis that CSCs represent a small subpopulation of cells within solid or non-solid tumors. Highly purified LCSCs (>96%) were subsequently obtained and formed colonies in the second passage after a 3-week culture period, with the identity of the LCSCs confirmed by their differentiation potential, soft-agar colony formation, and surface-marker expression.

Given that an overlap likely exists between CD133<sup>+</sup> and other cell-surface phenotypes of LCSCs, including EpCAM<sup>+</sup> (12), possibly due to tumor heterogeneity, LCSCs may not be sensitive to a single CSC-specific drug. Previous studies reported that Sal and OSM have each demonstrated anti-LCSC effects *in vivo* and *in vitro* via their distinct

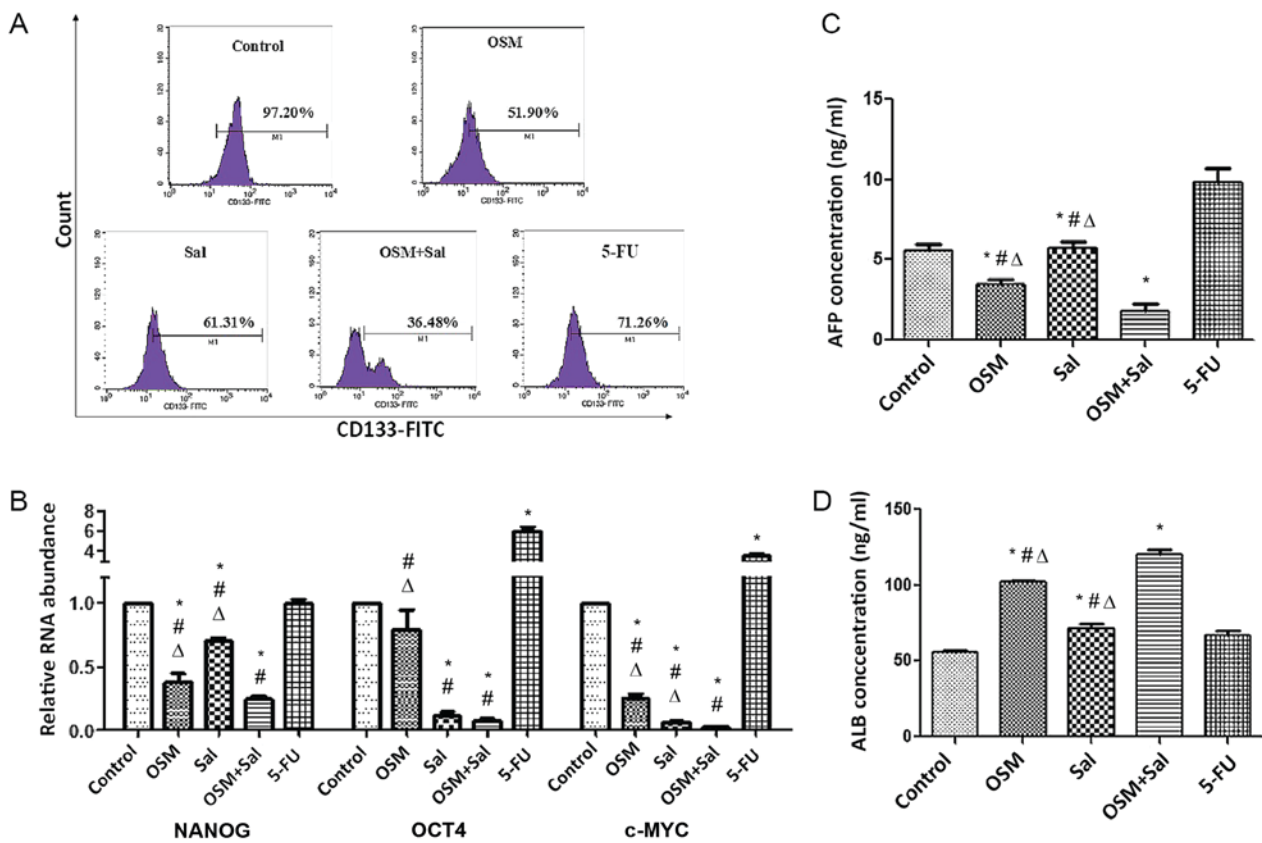


Figure 5. OSM and Sal induce expression of LCSC differentiation-related markers. (A) Fraction of LCSCs expressing CD133 after treatment with OSM, Sal, or both according to flow cytometric analysis. (B) Real-time quantitative reverse transcription polymerase chain reaction analysis of *NANOG*, *OCT4* and *c-MYC* mRNA expression in LCSCs treated with OSM, Sal, or both. Detection of (C) AFP and (D) ALB levels in the culture supernatant of LCSCs treated with OSM, Sal, or both by enzyme linked immunosorbent assay. OSM (10 ng/ml), Sal (1  $\mu$ M), or both (10 ng/ml OSM + 1  $\mu$ M Sal) were used in the experiments. Cells treated with 1  $\mu$ g/ml 5-FU served as the positive controls, and culture medium was used as a negative control. Data represent the mean  $\pm$  standard deviation. \* $P$ <0.05, compared with the control; # $P$ <0.05, compared with 5-FU,  $\Delta P$ <0.05, compared with the combination (OSM + Sal). OSM, oncostatin M; Sal, salinomycin; LCSC, liver cancer stem cell; AFP,  $\alpha$ -fetoprotein; ALB, albumin; 5-FU, 5-fluorouracil.

molecular pathways (10,12,13,24). In the present study, we assessed and compared the effects of treatment with Sal and OSM individually and in combination on LCSCs. The results revealed that LCSC proliferation was inhibited by Sal, OSM, and their combinatorial treatment, although the latter had a more potent effect. This was also true for induction of LCSC apoptosis and differentiation. Apoptosis resistance is a major factor associated with tumorigenesis and drug resistance (25). Caspase-3 is a downstream executioner caspase associated with the apoptotic process and that mediates protein cleavage of procaspases 3, 6, 7 and 9, as well as other caspase substrates important to the molecular mechanisms of apoptosis. Previous studies revealed that Sal induced caspase-mediated cell death in ovarian epithelial carcinoma, lung cancer cell lines, nasopharyngeal carcinoma, and colorectal CSCs (26-29). In the present study, enhanced early apoptosis of LCSCs after combination treatment with OSM and Sal was observed, according to JC-1 and Annexin V-FITC assays and caspase-3 activity, which suggested induction of apoptosis through the mitochondrial pathway. However, a more detailed investigation of the underlying mechanism of apoptosis in this context is required.

Stem cell-related transcription factors, such as OCT4, NANOG, and c-MYC, play critical roles in maintaining stemness and regulating downstream genes involved in

self-renewal and differentiation. Recently, the genes encoding these proteins were linked with abnormal growth and oncogenic transformation and have frequently been reported as overexpressed in human cancers (3). In the present study, we found significant reductions in the *OCT4*, *NANOG*, and *c-MYC* mRNA expression in LCSCs treated with the drug combination as compared with OSM or Sal treatment alone or results from the 5-FU group, suggesting an enhanced antiproliferative effect elicited by the drug combination on LCSCs. Moreover, combination treatment suppressed LCSC migration and invasion according to Transwell assays, possibly due in part to downregulated signaling associated with the focal adhesive kinase and extracellular signal-regulated kinase 1/2 pathways (14). ALB is produced by hepatocytes and represents a significant marker of hepatocyte differentiation; however, it is produced at lower levels in liver cancer cells. Conversely, AFP is expressed in liver cancer cells and represents a highly effective marker of liver cancer. In the present study, we observed decreased AFP levels and increased ALB levels following treatment with OSM or Sal alone and also after combination treatment, indicating induction of LCSC differentiation toward hepatocytes, although more pronounced effects were observed following treatment with OSM alone and both drugs. Similarly, OSM used along with hepatocyte growth factor

induced the differentiation of human mesenchymal stem cells from various sources into functional hepatocyte-like cells (16,30). Although the underlying mechanism remains unclear, one hypothesis suggests that OSM modulates liver cancer differentiation via the C-X-C chemokine receptor type 7/extracellular signal-regulated kinase/hepatocyte nuclear factor 4 $\alpha$  cascade (31).

In conclusion, the enhanced capability of the drug combination of OSM and Sal in suppressing LCSC proliferation and invasion, as well as its ability to induce early stage apoptosis and LCSC differentiation, *in vitro* was revealed. A potential limitation of this study was the use of a CCK-8 assay to assess cell viability following treatment with Sal, which is known to affect mitochondrial function such as mitochondrial ion translocation and respiration (32-34). However, previously published studies have also employed this assay to determine cell viability following Sal treatment (35-38). Although *in vivo* studies are required to validate these findings, and drug toxicity and side effects need to be evaluated, our findings indicated that combination therapy with OSM and Sal represents an important first step in the development of drug-combination therapy for liver cancer treatment.

#### Acknowledgements

The authors acknowledge Dr Zi Yan from The First Hospital of Jilin University (Changchun, China) for language editing.

#### Funding

This study was supported by the Technology Development Plan of Jilin Province (no. 20160204036YY) and the Fundamental Research Funds for the Central Universities.

#### Availability of data and material

All data generated and/or analyzed during this study are included in this published article.

#### Authors' contributions

CF wrote the paper and supervised the experiments. CF and LW performed the experiments. GT, CZ, and YZ, and HX performed analysis and interpretation of the data, and MS and YW conceived and designed the experiments. YW reviewed and revised the paper. All authors read and approved the final version of the manuscript.

#### Ethics approval and consent to participate

Not applicable.

#### Patient consent for publication

Not applicable.

#### Competing interests

The authors declare that they have no competing interests.

#### References

1. Ferlay J, Soerjomataram I, Dikshit R, Eser S, Mathers C, Rebelo M, Parkin DM, Forman D and Bray F: Cancer incidence and mortality worldwide: Sources, methods and major patterns in GLOBOCAN 2012. *Int J Cancer* 136: E359-E386, 2015.
2. Jordan CT, Guzman ML and Noble M: Cancer stem cells. *N Engl J Med* 355: 1253-1261, 2006.
3. Naujokat C and Steinhart R: Salinomycin as a drug for targeting human cancer stem cells. *J Biomed Biotechnol* 2012: 950658, 2012.
4. Bexell D, Gunnarsson S, Siesjö P, Bengzon J and Darabi A: CD133+ and nestin+ tumor-initiating cells dominate in N29 and N32 experimental gliomas. *Int J Cancer* 125: 15-22, 2009.
5. Gupta PB, Onder TT, Jiang G, Tao K, Kuperwasser C, Weinberg RA and Lander ES: Identification of selective inhibitors of cancer stem cells by high-throughput screening. *Cell* 138: 645-659, 2009.
6. Zhi QM, Chen XH, Ji J, Zhang JN, Li JF, Cai Q, Liu BY, Gu QL, Zhu ZG and Yu YY: Salinomycin can effectively kill ALDH(high) stem-like cells on gastric cancer. *Biomed Pharmacother* 65: 509-515, 2011.
7. Dong TT, Zhou HM, Wang LL, Feng B, Lv B and Zheng MH: Salinomycin selectively targets CD133+ cell subpopulations and decreases malignant traits in colorectal cancerlines. *Ann Surg Oncol* 18: 1797-1804, 2011.
8. Kim KY, Yu SN, Lee SY, Chun SS, Choi YL, Park YM, Song CS, Chatterjee B and Ahn SC: Salinomycin-induced apoptosis of human prostate cancer cells due to accumulated reactive oxygen species and mitochondrial membrane depolarization. *Biochem Biophys Res Commun* 413: 80-86, 2011.
9. He L, Wang F, Dai WQ, Wu D, Lin CL, Wu SM, Cheng P, Zhang Y, Shen M, Wang CF, *et al.*: Mechanism of action of salinomycin of growth and migration in pancreatic cancer cell line. *Pancreatol* 13: 72-78, 2013.
10. Wang F, He L, Dai WQ, Xu YP, Wu D, Lin CL, Wu SM, Cheng P, Zhang Y, Shen M, *et al.*: Salinomycin inhibits proliferation and induces apoptosis of human hepatocellular carcinoma cells *in vitro* and *in vivo*. *PLoS One* 7: e50638, 2012.
11. Park SY, Gönen M, Kim HJ, Michor F and Polyak K: Cellular and genetic diversity in the progression of *in situ* human breast carcinomas to an invasive phenotype. *J Clin Invest* 120: 636-644, 2010.
12. Yamashita T, Honda M, Nio K, Nakamoto Y, Yamashita T, Takamura H, Tani T, Zen Y and Kaneko S: Oncostatin m renders epithelial cell adhesion molecule-positive liver cancer stem cells sensitive to 5-Fluorouracil by inducing hepatocytic. *Cancer Res* 70: 4687-4697, 2010.
13. Zheng H, Pomyen Y, Hernandez MO, Li C, Livak F, Tang W, Dang H, Greten TF, Davis JL, Zhao Y, *et al.*: Single cell analysis reveals cancer stem cell heterogeneity in hepatocellular carcinoma. *Hepatology* 68: 127-140, 2018.
14. Sun J, Luo Q, Liu L, Yang X, Zhu S and Song G: Salinomycin attenuates liver cancer stem cell motility by enhancing cell stiffness and increasing F-actin formation via the FAK-ERK1/2 signalling pathway. *Toxicology* 384: 1-10, 2017.
15. Tanaka M and Miyajima A: Oncostatin M, a multifunctional cytokine. *Rev Physiol Biochem Pharmacol* 149: 39-52, 2003.
16. Nakamura K, Nonaka H, Saito H, Tanaka M and Miyajima A: Hepatocyte proliferation and tissue remodeling is impaired after liver injury in oncostatin M receptor knockout mice. *Hepatology* 39: 635-644, 2004.
17. Larrea E, Aldabe R, Gonzalez I, Segura V, Sarobe P, Echeverria I and Prieto J: Oncostatin M enhances the antiviral effects of type I interferon and activates immunostimulatory functions in liver epithelial cells. *J Virol* 83: 3298-3311, 2009.
18. Lepiller Q, Abbas W, Kumar A, Tripathy MK and Herbein G: HCMV activates the IL-6-JAK-STAT3 axis in HepG2 cells and primary human hepatocytes. *PLoS One* 8: e59591, 2013.
19. Livak KJ and Schmittgen TD: Analysis of relative gene expression data using real-time quantitative PCR and the 2(-Delta Delta C(T)) method. *Methods* 25: 402-408, 2001.
20. Ajani JA, Song S, Hochster HS and Steinberg IB: Cancer stem cells: The promise and the potential. *Semin Oncol* 42 (Suppl): 3-17, 2015.
21. Ma S, Chan KW, Hu L, Lee TK, Wo JY, Ng IO, Zheng BJ and Guan XY: Identification and characterization of tumorigenic liver cancer stem/progenitor cells. *Gastroenterology* 132: 2542-2556, 2007.
22. Ma S, Lee TK, Zheng BJ, Chan KW and Guan XY: CD133+ HCC cancer stem cells confer chemoresistance by preferential expression of the Akt/PKB survival pathway. *Oncogen* 27: 1749-1758, 2008.

23. Lan X, Wu YZ, Wang Y, Wu FR, Zang CB, Tang C, Cao S and Li SL: CD133 silencing inhibits stemness properties and enhances chemoradiosensitivity in CD133-positive liver cancer stem cells. *Int J Mol Med* 31: 315-324, 2013.
24. Kong N, Zhang XM, Wang HT, Mu XP, Han HZ and Yan WQ: **Inhibition of growth and induction of differentiation of SMMC-7221 human hepatocellular carcinoma cells by oncostatin M.** *Asian Pac J Cancer Prev* 14: 747-752, 2013.
25. Lee S and Schmitt CA: Chemotherapy response and resistance. *Curr Opin Genet Dev* 13: 90-96, 2003.
26. Kaplan F and Teksen F: Apoptotic effects of salinomycin on human ovarian cancer cell line (ovcar-3). *Tumor Biol* 37: 3897-3903, 2016.
27. Arafat K, Iratni R, Takahashi T, Parekh K, Al Dhaheri Y, Adrian TE and Attoub S: Inhibitory effects of salinomycin on cell survival, colony growth, migration, and invasion of human non-small cell lung cancer a549 and Inm35: Involvement of nag-1. *PLoS One* 8: e66931, 2013.
28. Wu D, Zhang Y, Huang J, Fan Z, Shi F and Wang S: Salinomycin inhibits proliferation and induces apoptosis of human nasopharyngeal carcinoma cell and suppresses tumor growth in vivo. *Biochem Biophys Res Commun* 443: 712-717, 2014.
29. Zhang C, Tian Y, Song F, Fu C, Han B and Wang Y: Salinomycin inhibits the growth of colorectal carcinoma by targeting tumor stem cells. *Oncol Rep* 34: 2469-2476, 2015.
30. Lee KD, Kuo TK, Whang-Peng J, Chung YF, Lin CT, Chou SH, Chen JR, Chen YP and Lee OK: In vitro hepatic differentiation of human mesenchymal stem cells. *Hepatology* 40: 1275-1284, 2004.
31. Xue TC, Jia QA, Bu Y, Chen RX, Cui JF, Tang ZY and Ye SL: CXCR7 correlates with the differentiation of hepatocellular carcinoma and suppresses HNF4 $\alpha$  expression through the ERK pathway. *Oncol Rep* 32: 2387-2396, 2014.
32. Mitani M, Yamanishi T, Miyazaki Y and Otake N: Salinomycin effects on mitochondrial ion translocation and respiration. *Antimicrob Agents Chemother* 9: 655-660, 1976.
33. Managò A, Leanza L, Carraretto L, Sassi N, Grancara S, Quintana-Cabrera R, Trimarco V, Toninello A, Scorrano L, Trentin L, et al: **Early effects of the antineoplastic agent salinomycin on mitochondrial function.** *Cell Death Dis* 6: e1930, 2015.
34. Klose J, Stankov MV, Kleine M, Ramackers W, Panayotova-Dimitrova D, Jäger MD, Klempnauer J, Winkler M, Bektas H, Behrens GM and Vondran FW: Inhibition of autophagic flux by salinomycin results in anti-cancer effect in hepatocellular carcinoma cells. *PLoS One* 9: e95970, 2014.
35. Fu YZ, Yan YY, He M, Xiao QH, Yao WF, Zhao L, Wu HZ, Yu ZJ, Zhou MY, Lv MT, et al: Salinomycin induces selective cytotoxicity to MCF-7 mammosphere cells through targeting the Hedgehog signaling pathway. *Oncol Rep* 35: 912-922, 2016.
36. Zhu LQ, Zhen YF, Zhang Y, Guo ZX, Dai J and Wang XD: Salinomycin activates AMP-activated protein kinase-dependent autophagy in cultured osteoblastoma cells: A negative regulator against cell apoptosis. *PLoS One* 8: e84175, 2013.
37. Zhang Y, Zuo Y, Guan Z, Lu W, Xu Z, Zhang H, Yang Y, Yang M, Zhu H and Chen X: Salinomycin radiosensitizes human nasopharyngeal carcinoma cell line CNE-2 to radiation. *Tumour Bio* 37: 305-311, 2016.
38. Mao J, Fan S, Ma W, Fan P, Wang B, Zhang J, Wang H, Tang B, Zhang Q, Yu X. et al: Roles of Wnt/ $\beta$ -catenin signaling in the gastric cancer stem cells proliferation and salinomycin treatment. *Cell Death Dis* 5: e1039, 2014.



This work is licensed under a Creative Commons Attribution-NonCommercial-NoDerivatives 4.0 International (CC BY-NC-ND 4.0) License.